Robustness of nuclear core activity reconstruction by data assimilation

Bertrand Bouriquet [a,*], Jean-Philippe Argaud [a,b], Patrick Erhard [b], Sébastien Massart [a], Angélique Ponçot [b], Sophie Ricci [a], Olivier Thual [a,c]

[a] Sciences de l'Univers au CERFACS, URA CERFACS/CNRS No. 1875, 42 avenue Gaspard Coriolis, F-31057 Toulouse Cedex 01, France
[b] Electricité de France, 1 avenue du Général de Gaulle, F-92141 Clamart Cedex, France
[c] Université de Toulouse, INPT, UPS, IMFT, Allée Camille Soula, F-31400 Toulouse, France

A B S T R A C T

We apply a data assimilation technique, inspired from meteorological applications, to perform an optimal reconstruction of the neutronic activity field in a nuclear core. Both measurements and information coming from a numerical model are used. We first study the robustness of the method when the amount of measured information decreases. We then study the influence of the nature of the instruments and their spatial repartition on the efficiency of the field reconstruction.

* Corresponding author.
E-mail address: bertrand.bouriquet@cerfacs.fr (B. Bouriquet).

Keywords:
Data assimilation
Schur complement
Neutronic
Activities reconstruction
Nuclear in-core measurements

1. Introduction

In this paper, we focus on the efficiency of a neutronic field reconstruction procedure with data assimilation when the number and the repartition of the available instruments is varying. The data assimilation technique used for this reconstruction allows to combine, in an optimal and consistent way, information coming either from measurements or from a numerical model.

Data assimilation methods are not commonly used in nuclear core physics [1], contrary to meteorology or oceanography [2–4]. The procedure proposed here is the same as the one meteorologists use to obtain high accuracy meteorological reconstructed fields in time and space. This is the case, for example, of the commonly used meteorological re-analysis data set ERA-40 [5] among others [6,7].

One of the main advantages of data assimilation is that it takes into account every kind of heterogeneous information within the same framework. Moreover, this method has a formalism that allows to adapt itself to instrument configuration change. We exploit this last property here, to study the quality of the reconstructed activity field as a function of the number of available measurements. A major point in this study is to estimate the instrumented system robustness in the framework of a data assimilation reconstruction procedure. Moreover, such a study also informs about the effect of instrumentation design within a nuclear core and the resilience to instrument removal.

In this paper, we first detail the data assimilation method and how it addresses field reconstruction. To evaluate the influence of the number of instruments on the activity field reconstruction, the repeated application of the method faces some huge computational issues. These difficulties are overcome using a matrix inversion method based on the Schur complement. A detailed presentation of this method is presented in Appendix A. First we present the results on a standard case with synthetic measurements and comment on them. To get a better understanding, we extend the results to other instrumental repartitions and other error settings. This allows us to give some conclusions on the error and instrument repartition effects in activity field reconstruction using data assimilation.

2. Data assimilation

We briefly introduce the useful data assimilation key points to understand their use as applied in Refs. [8–10]. Data assimilation is a wider domain and these techniques are, for example, the keys of the meteorological operational forecasts nowadays [11]. Thus through advanced data assimilation methods weather forecasting has been drastically improved during the last 30 years. All the available data, such as satellite measurements as well as sophisticated numerical models, are used.

The ultimate goal of data assimilation methods is to estimate the inaccessible true value of the system state, $\mathbf{x}^t$ where the t index

doi:10.1016/j.nima.2010.09.180

stands for "true state" in the so-called "control space". The basic idea is to combine information from an *a priori* on the state of the system (usually called $\mathbf{x}^b$, with b for "background"), and measurements (referenced as $\mathbf{y}^o$). The background is usually the result of numerical simulations, but can also be derived from any *a priori* knowledge. The result of data assimilation is called the analysis, denoted by $\mathbf{x}^a$, and it is an estimation of the true state $\mathbf{x}^t$ we want to approximate.

The control and observation spaces are not necessarily the same, and a bridge between them needs to be built. This is the observation operator H, that transforms values from the space of the background into the space of observations. For our data assimilation purpose we will use its linearisation $\mathbf{H}$ around the background. The inverse operation going from observation increments to background increments is given by the transpose $\mathbf{H}^T$ of $\mathbf{H}$.

Two other ingredients are necessary. The first is the covariance matrix of observation errors, defined as $\mathbf{R} = E[(\mathbf{y}^o - H(\mathbf{x}^t)) \cdot (\mathbf{y}^o - H(\mathbf{x}^t))^T]$ where $E[\cdot]$ is the mathematical expectation. It can be obtained from the known errors on unbiased measurements which means $E[\mathbf{y}^o - H(\mathbf{x}^t)] = 0$. The second is the covariance matrix of background errors, defined as $\mathbf{B} = E[(\mathbf{x}^b - \mathbf{x}^t) \cdot (\mathbf{x}^b - \mathbf{x}^t)^T]$. It represents the error on the *a priori* state, assuming it to be unbiaised following the $E[\mathbf{x}^b - \mathbf{x}^t] = 0$ no bias property. There are many ways to get this *a priori* state and background error matrices. However, these matrices are commonly the output of a model and an evaluation of accuracy or the result of expert knowledge.

It can be proved, within this formalism that the Best Linear Unbiased Estimator (BLUE) $\mathbf{x}^a$, under the linear and static assumptions, is given by the following equation:

$$\mathbf{x}^a = \mathbf{x}^b + \mathbf{K}(\mathbf{y}^o - H\mathbf{x}^b) \tag{1}$$

where $\mathbf{K}$ is the gain matrix:

$$\mathbf{K} = \mathbf{B}\mathbf{H}^T(\mathbf{H}\mathbf{B}\mathbf{H}^T + \mathbf{R})^{-1}. \tag{2}$$

Moreover, we can get the analysis error covariance matrix $\mathbf{A}$, characterising the analysis errors $\mathbf{x}^a - \mathbf{x}^t$. This matrix can be expressed from $\mathbf{K}$ as

$$\mathbf{A} = (\mathbf{I} - \mathbf{K}\mathbf{H})\mathbf{B} \tag{3}$$

where $\mathbf{I}$ is the identity matrix.

It is worth noting that solving Eq. (1) is, if the probability distribution is Gaussian, equivalent to minimising the following function $J(\mathbf{x})$, $\mathbf{x}^a$ being the optimal solution:

$$J(\mathbf{x}) = (\mathbf{x} - \mathbf{x}^b)^T\mathbf{B}^{-1}(\mathbf{x} - \mathbf{x}^b) + (\mathbf{y}^o - \mathbf{H}\mathbf{x})^T\mathbf{R}^{-1}(\mathbf{y}^o - \mathbf{H}\mathbf{x}). \tag{4}$$

This minimisation procedure is known in data assimilation as 3D-Var methodology [8].

3. Data assimilation implementation

The framework of this study is the standard configuration of a 900 MWe nuclear Pressurized Water Reactor (PWR900). To perform data assimilation, both simulation code and data are needed. For the simulation code, the EDF experimental calculation code for nuclear core COCAGNE in a standard configuration is used. The description of the basic features of this model is given in Section 3.1.

To have a good understanding of the instrumentation effect, we want to study the various kinds of configurations, even some that do not exist operationally and so cannot be tested experimentally. For that purpose, synthetic data are used that allow to have a homogeneous approach all along the document. Synthetic data are generated from a model simulation, filtered through an instrument model, and noised according to a predefined measurement error density function (usually of Gaussian type).

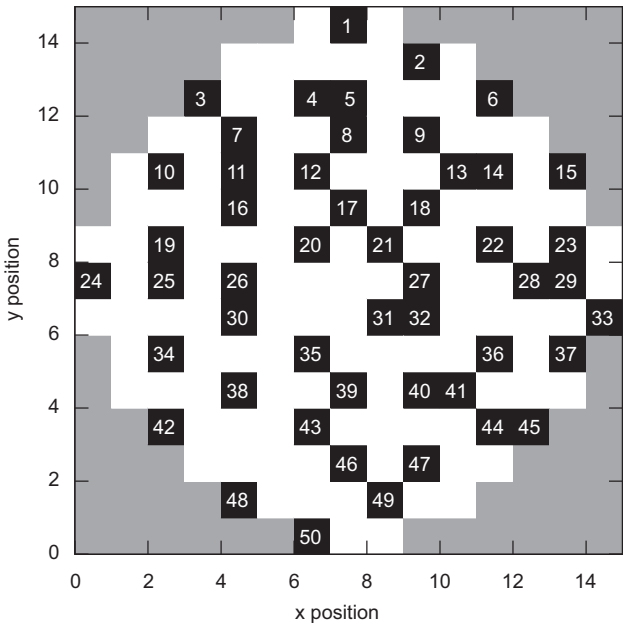

Fig. 1. The positions of MFC instruments in the nuclear core are localised in assemblies in black within the horizontal slice of the core. The assemblies without instrument are marked in white and the reflector, out of the reactive core, is in gray.

In the present case, we study the activity field reconstruction. A horizontal slice of a PWR900 core is represented in Fig. 1. There is a total of 157 vertical assemblies within this core. Among these assemblies, 50 are instrumented with Mobiles Fissions Chambers (MFC). These assemblies are divided vertically in 29 vertical levels. Thus, the size of the control $\mathbf{x}$ is 4553 (157×29). The size of the observation vector $\mathbf{y}^o$ is 1450 (50×29).

3.1. Brief description of the nuclear core model

The aim of a neutronic code like COCAGNE is to evaluate the neutronic activity field and all associated values within the nuclear core. This field depends on the position in the core and on the neutron energy. To do such an evaluation, the population of neutrons are divided into several groups of energy. In the present case only two groups are taken into account, leading to the neutronic flux described by $\Phi = (\Phi_1, \Phi_2)$ (even if the present code has no limit for the group number). The material properties depend on the position in the core, and the neutronic flux Φ is identified by solving two-group neutronic diffusion equations described by

$$\begin{cases} -\mathrm{div}(D_1 \mathrm{grad}\Phi_1) + (\Sigma_{a1} + \Sigma_r)\Phi_1 = \frac{1}{k}(\nu_1\Sigma_{f1}\Phi_1 + \nu_2\Sigma_{f2}\Phi_2) \\ -\mathrm{div}(D_2 \mathrm{grad}\Phi_2) + \Sigma_{a2}\Phi_2 - \Sigma_r\Phi_1 = 0 \end{cases} \tag{5}$$

where all the quantities and the derivatives (except k) depend on the position in the core, k is the effective neutron multiplication factor, Σ_r is the scattering cross-section from group 1 to group 2, 1 and 2 are the group indexes, and for each group, Φ is the neutron flux, Σ_a is the absorption cross-section, D is the diffusion coefficient, $\nu\Sigma_f$ is the corrected fission cross-section.

The cross-sections also depend implicitly on the concentration of boron, which is a substance added in the water used for the primary circuit to control the neutronic fission reaction, through a feedback supplementary model. This model takes into account the temperature of the materials and of the neutron moderator, given by external thermal and thermo-hydraulic models. A detailed description of the core physic and numerical solving can be found in Ref. [12].

The overall numerical resolution consists in searching for boron concentration such that the eigenvalue k is equal to 1, which means that the nuclear power production is stable and self-sustaining. It is named critical boron concentration computation.

The activity in the core is obtained through a combination of the fluxes $\Phi = (\Phi_1, \Phi_2)$, given on the chosen mesh of the core. Using homogeneous materials for each assembly (for example 157 in a PWR900 reactor), and choosing a vertical mesh compatible with the core (usually 29 vertical levels), this result in a field of activity of size $157 \times 29 = 4553$ that cover all the core.

3.2. The observation operator H

The H observation operator is the composition of a selection and of a normalisation procedure. The selection procedure extracts the values corresponding to effective measurement among the values of the model space. The normalisation procedure is a scaling of the value with respect to the geometry and power of the core. The overall operation is non-linear. However, with a range of value compatible with assimilation procedure, we can calculate the linear associated operator **H**. This observation matrix is a (4553×1450) matrix.

3.3. The background error covariance matrix B

The **B** matrix represents the covariance between the spatial errors for the background. In order to get them, we estimate them as the product of a correlation matrix **C** by a normalisation factor.

The correlation **C** matrix is built using a positive function that defines the correlations between instruments with respect to a pseudo-distance in model space. Positive functions have the property (via Bochner theorem) to build a symmetric defined positive matrix when they are used as a matrix generator [13,14]. In the present case, Second Order Auto-Regressive (SOAR) function is used to prescribe the **C** matrix. In such a function, the amount of correlation depends upon the Euclidean distance between spatial points. The radial and vertical correlation lengths (L_r and L_z respectively, associated to the radial r coordinate and the vertical z coordinate) have different values, which means that we are dealing with a global pseudo euclidean distance. The used function can be expressed as follows:

$$C(r,z) = \left(1 + \frac{r}{L_r}\right)\left(1 + \frac{|z|}{L_z}\right)\exp\left(-\frac{r}{L_r} - \frac{|z|}{L_z}\right). \tag{6}$$

The matrix obtained by Eq. (6) is a correlation matrix. It is then multiplied by a suitable variance coefficient to get a covariance matrix. This coefficient is obtained by statistical study of the difference between model and measurements in the real case. In our case, the size of the **B** matrix is related to the size of model space so it is (4553×4553).

3.4. The observation error covariance matrix R

The observation error covariance matrix **R** is approximated by a diagonal matrix. This means that it is assumed that no significant correlation exists between the measurement errors of the MFC. The usual modelling is to take those values as a percentage of the observation. This can be expressed as

$$\mathbf{R}_{jj} = (\alpha y_j^o)^2, \quad \forall j. \tag{7}$$

The parameter α is fixed according to the accuracy of the measurement and the representative error associated to the instrument. The size of the **R** matrix is related to the size of observation space, so it is (1450×1450).

4. General results on instrument removal

To test the robustness, many BLUE calculations need to be done to evaluate the results' quality with instruments configuration modifications. We want to have an evaluation of the quality of reconstruction as a function of the number of instruments, with a significant statistical result. To efficiently perform these numerous computations, a specific method using Schur complement was developed. The details of this new method are reported in Appendix A.

Here, we are interested in the evaluation of the quality of the analysis $\mathbf{x}^a$ as a function of the amount of provided information. To quantify this effect we make a statistic of 200 scenarios of instruments removal. We make these statistics on several hypotheses, starting from a complete instrument configuration, and then removing instruments two by two until none remains. The calculations are done on the basis of the algorithm and hypothesis on the data assimilation described previously.

To quantify the impact of removed instruments on the analysis, we look at the percentage quantity ν defined as follows:

$$\nu = 100\frac{||\mathbf{y}^o_{ref} - H\mathbf{x}^b|| - ||\mathbf{y}^o_{ref} - H\mathbf{x}^a||}{||\mathbf{y}^o_{ref} - H\mathbf{x}^b|| - ||\mathbf{y}^o_{ref} - H\mathbf{x}^a_{ref}||} \tag{8}$$

where $\mathbf{x}^a_{ref}$ corresponds to the analysis when no instrument is removed (this is the best estimation possible with respect to the information available on the system), and where $\mathbf{y}^o_{ref}$ and H are the reference observations and observation operator used to build $\mathbf{x}^a_{ref}$. H stands for the observation operator when no instrument is removed. This criterium, which is based on the norm of the innovation vector $\mathbf{y}^o_{ref} - H\mathbf{x}^b$, focuses on measurements. Since $||\mathbf{y}^o_{ref} - H\mathbf{x}^a||$ is greater than $||\mathbf{y}^o_{ref} - H\mathbf{x}^a_{ref}||$ (best estimate) and smaller than $||\mathbf{y}^o_{ref} - H\mathbf{x}^b||$ (innovation), ν is a measure of the quality of the analysis.

Such a definition has several advantages. First of all, the limits of this function are interesting. On the one hand, the limit when no instrument is removed is 100%. On the other hand, the limit when all instruments are removed is 0%. With such a formula we can compare the variation of the information on a unique scale. If we obtain some value above the limit of 100%, this means that the parameterisation of data assimilation was not done correctly.

The interest in using this formula is that it can be applied directly as well as to experimental and synthetic data without any change.

In Fig. 2 are presented the results of the quantity ν as a function of the number of removed instruments.

As expected, the relative quality of reconstruction decreases as a function of the number of instruments removed. However within this decrease, three phases can be seen:

1. A first phase of slow decreasing until we removed roughly 20 instruments. This phase is rather clear and can be fitted by a linear regression with a slope of -1.64 (*arbitrary unit (a.u.) per instrument*). The fit is shown in (green) dash line in Fig. 2.
2. After 20 instruments are removed the decreasing speed of the slope increases. The second linear fit has a slope of -2.28 (*a.u. per instrument*). This fit is shown in (blue) dotted line in Fig. 2.
3. Beyond 40 instruments' removal, we reach a third phase of stagnation, then a brutal decrease to 0, the limit value imposed by Eq. (8).

This characteristic behaviour can be seen in several cases that we studied. We have also noticed it on real measurements [15,16]. The transition between the two first decreasing phases is specially strong when we do the analysis using real measurements.

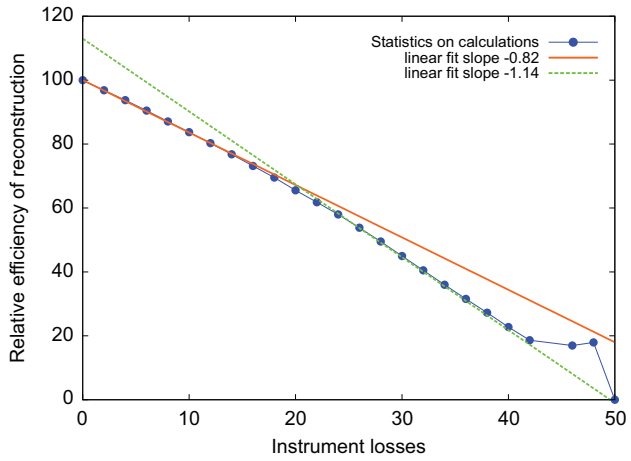

Fig. 2. The plain curve represents the value ν given by Eq. (8) as a function of the number of instruments removed. These results come from a typical PWR900 instrument location. The other two lines are linear regression both corresponding to a decreasing regime.

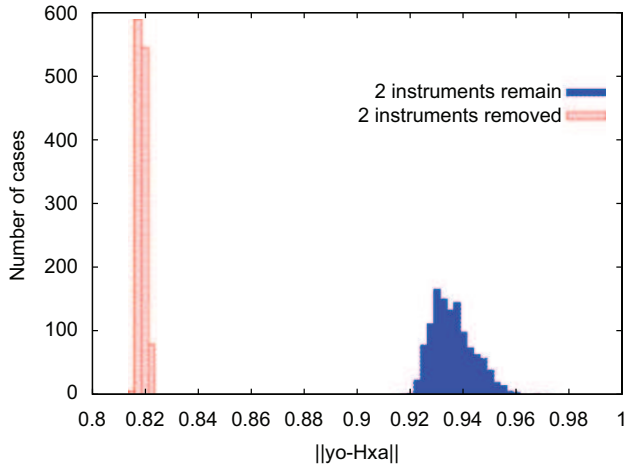

Fig. 3. Distribution of the norms of $||\mathbf{y}^o - \mathbf{H}\mathbf{x}^a||$ for all the cases where only two instruments are suppressed or two instruments remain in the instrument network on a PWR900 reactor.

First, we explain why the third phase is marked by a stagnation of the mean value of $||\mathbf{y}^o - \mathbf{H}\mathbf{x}^a||$ over the set of removal scenarios taken into account. To understand that effect, we work on both the cases where two instruments are removed (*i.e.*48 are remaining), and on where two instruments are remaining. On those two cases, at most 1225 scenarios are possible, corresponding to the C_2^{50} combinations. Using the hybrid Schur method, we can calculate all those cases with rather cheap computing time to obtain good statistics. We plotted the distribution of the value of $||\mathbf{y}^o - \mathbf{H}\mathbf{x}^a||$ over all the scenarios in Fig. 3.

In Fig. 3 we notice a big difference between the two distributions plotted, that correspond to the cases where two instruments are removed (*i.e.*48 remain) or two are remaining.

The shifting of the mean value between those two extreme cases is logical, as available information is dramatically changing. However, the shape of the distribution is also vastly changing. We move from a very sharp distribution, when 48 instruments are remaining, to a rather broad one when only two instruments are remaining.

The first interesting point of this shape change is that all the instruments do not have the same influence on the activity field reconstruction. To understand better this effect let us assume that all the instruments are equivalent. In this case, as the number of scenarios present in the two distributions of Fig. 3 are the same, only a shifting of the mean value should be seen. However we have not only a translation of the distribution but also a broadening. Thus, there is a non-equivalence of instruments within the data assimilation procedure, in terms of marginal information assigned to each instrument, depending on its location in the core.

The second point of interest is that the broadening of the distribution is asymmetric. The distribution extends towards the higher values of norm. This effect explains the stagnation of the ν quantity when few instruments remain. The source of stagnation is the discrepancy between the most probable value of the distribution and the mean value of the distribution which is higher. The most probable value leads to a decrease without stagnation. However, looking at the mean value (that has more physical meaning), we see that this one stagnates due to the asymmetric broadening that compensates the overall decrease in mean value.

Now the origin of the two slopes in decreasing the information represented by Fig. 2 will be investigated. The repartition of the instruments in a standard PWR900 is very complex as shown in Fig. 1. This complexity of the repartition does not make the situation easy to understand. Thus, we want to study the case on a simpler repartition of the instrumentation to see if the effect of the two phases decreasing persists.

5. Repartition effects in instrument removal

An artificial set of instrument positions is presented in Fig. 4. The core geometry and assemblies configuration is the same as a PWR900, however the instruments are located regularly on a Cartesian map.

Within this configuration, only 40 MFC are used, which is slightly less than 50 of the standard PWR configuration presented in Fig. 1. With this repartition, we do the same analysis as on the previous one. The evolution on ν as a function of the number of removed instruments is plotted in Fig. 5.

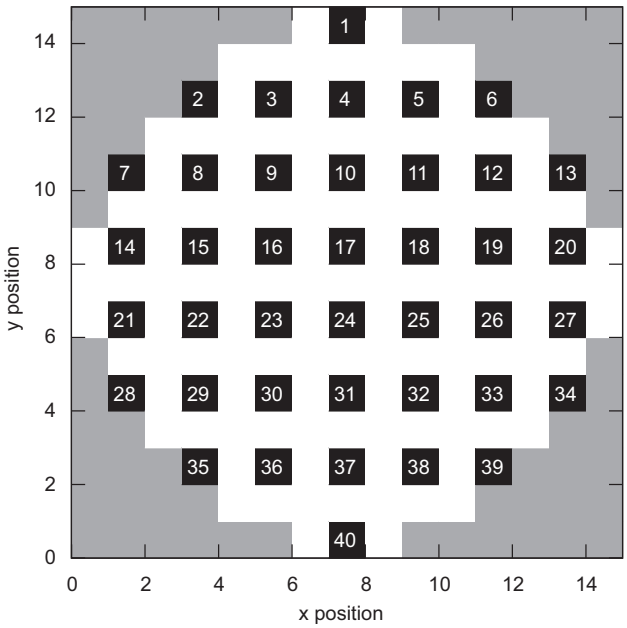

Fig. 4. The MFC instruments within the nuclear core are localised in assemblies in black within the horizontal slice of the core. The assemblies without instruments are marked in white and the reflector is in gray.

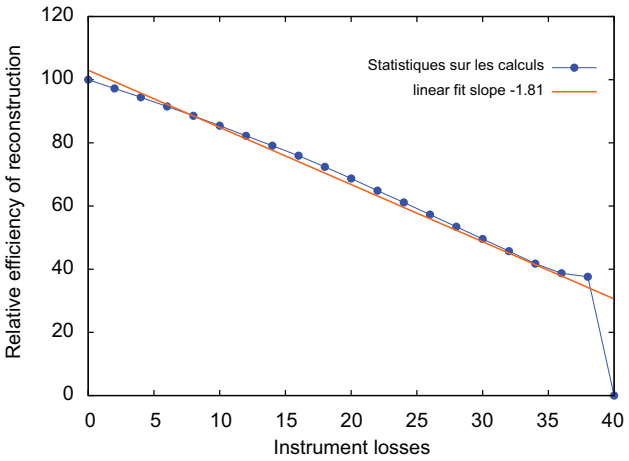

Fig. 5. The plain curve represents the value ν given by Eq. (8) as a function of the number of instruments removed. This results come from a regular instruments location in a PWR900. The dashed line represents the linear fit of the steady part of the curve.

In Fig. 5, the quality of the activity reconstruction decreases quasi-linearly as a function of the number of removed instruments. This goes on until we reach the stagnation phase. It appears, comparing Fig. 5 to Fig. 2 that the variation of the decrease slope is related to the geometrical repartition of the instruments. Such a uniform linear decrease can be observed also in several other rather geometrically regular repartitions, as one with repartition on a diagonal line. Some of the repartitions have densities of instruments close to the one of the standard PWR900, which do not change the overall behaviour.

Looking at the slope factor of the linear fit, we notice that the one with regular MFC repartition (Fig. 5) is in the range of the slopes obtained with standard MFC repartition (Fig. 2).

Thus the removal or fault resilience of the instrument set seems to depend on the transition point between the two decreasing steps. In the lower range of instrumental density, it is better to have a regular repartition, and in the higher one, it is better to have a complex ad hoc repartition. In real PWR900 nuclear core, because the set of instruments is fixed at a high density level, these results indicate that it is more robust to have an ad hoc repartition of the instruments as for now.

6. Conclusion

We proposed and studied here an original method to test how the neutronic activity field reconstruction by data assimilation is tolerant to information removal. The core of the reconstruction method is based on data assimilation, which is widely used in earth sciences, and allows a very good reconstruction of the activity all over the nuclear core. A hybrid method for fast matrix inversion partially based on Schur complement allows the execution on numerous analysis from which statistical results are derived. For all these analyses, synthetic data are used to try non-experimental instrument repartitions, but similar results were established using real data. This application on real data prove both the reliability and the quality of the calculation code and the data assimilation methodology.

Using such advanced calculation methods, it was shown that the slopes of the reconstruction quality is mainly governed by repartition for the instruments. Depending on the chosen repartition, the decrease consists in two or three distinct phases. The ultimate stagnation phase in this decrease is governed by both statistical effect and heterogeneity of instruments influence.

The behaviour with two phases within the decreasing quality of the reconstruction as a function of the number of instruments removed is understood in terms of repartition effect, but not quantified. However, it can be seen as a phase transition between two states of instrumental configuration. The quantification of this transition is worth studying.

Appendix A. Schur complement method to optimise calculation

Within the BLUE assimilation method, the limiting factor in calculation time is the matrix inversions. In Eq. (2), the costly part is the inversion of the term:

$$\mathbf{M} = \mathbf{H}\mathbf{B}\mathbf{H}^T + \mathbf{R}. \tag{9}$$

The inversion cost on huge matrix as $\mathbf{M}$ (around 4000×4000 in the present case) was such that the time calculation of the above evaluation was extremely time-consuming. Then we had to optimise the computing cost.

We noticed that the calculations are more time-consuming when only few instruments are removed. In this case the $\mathbf{M}$ matrix is still huge.

Thus, the idea is to use the information obtained in the inversion of the full size matrix to shorten calculation, to calculate a smaller size matrix in a reasonable time. In this case, we want to calculate the new matrix as a perturbation of the original one. Such a method exists and exploits the Schur complement of the matrix.

We assume that we want to suppress some instruments to a given configuration. With respect to Eq. (2), we need to calculate a new matrix $\mathbf{K}_n$. The n index is standing for referring the new matrix we want to calculate. For that, according to Eq. (9), we have to determine a new matrix $\mathbf{M}_n$.

This determination of $\mathbf{M}_n$ is obtained from the knowledge of the invert of the matrix $\mathbf{M}_g$ calculated over all the instruments. The indices g is used to denote the reference global matrix we start from, $\mathbf{M}_g$, according to Eq. (9).

All the components of the new matrix $\mathbf{K}_n$ can be obtained by suppressing the lines and columns corresponding to the removed instruments in $\mathbf{M}_g$, inverting it and then multiplying this matrix by the corresponding $\mathbf{H}_n$ and $\mathbf{B}_n$. We notice that, in our case, we get $\mathbf{B}_n = \mathbf{B}_g$ as we do not affect the model space.

To make the demonstration easier, but without losing any generality, we can assume that the suppressed instruments correspond to the lower square of $\mathbf{M}_g$. If it is not the case, it is always possible to reorganise the matrix in such a way.

Now we put the $\mathbf{M}_g$ in a convenient form, separating the remaining measures from the removed ones. Assuming the starting matrix $\mathbf{M}_g$ is $m \times m$ and that we plan to suppress s measurements, we can write $\mathbf{M}_g$ in the following way:

$$\mathbf{M}_g = \begin{pmatrix} \mathbf{P}_g & \mathbf{Q}_g \\ \mathbf{R}_g & \mathbf{S}_g \end{pmatrix} \tag{10}$$

where:

- $\mathbf{P}_g$ contains the remaining measurements, and is a $p \times p$ matrix,
- $\mathbf{S}_g$ contains the suppressed measurement, and is a $s \times s$ matrix,
- $\mathbf{Q}_g$ and $\mathbf{R}_g$ represent the dependence between remaining measured and suppressed ones. In the particular case we are dealing with, we have $\mathbf{Q}_g^T = \mathbf{R}_g$. However, no further use of this property is done.

With such a decomposition, we got the equality $m = p + s$.

The $\mathbf{P}_g$ matrix corresponds to the remaining instruments, thus we have the following equality:

$$\mathbf{P}_g = \mathbf{M}_n. \tag{11}$$

The decomposition given in Eq. (10) is the one required to build the Schur complement of this matrix [17]. Under the condition that $\mathbf{P}_g$ can be inverted, the Schur complement is the following quantity:

$$\mathbf{S}_g - \mathbf{R}_g \mathbf{P}_g^{-1} \mathbf{Q}_g \tag{12}$$

and is noted $(\mathbf{M}_g/\mathbf{P}_g)$. This notation reads as Schur complement of $\mathbf{M}_g$ by $\mathbf{P}_g$.

Thus we look for a cheap way to calculate $\mathbf{P}_g^{-1}$ knowing $\mathbf{M}_g^{-1}$. For that, we use the Banachiewiz formula [17] that gives the invert of $\mathbf{M}_g$ as a function of $\mathbf{P}_g$, $\mathbf{Q}_g$, $\mathbf{R}_g$, $\mathbf{S}_g$ and $(\mathbf{M}_g/\mathbf{P}_g)$ matrices:

$$\mathbf{M}_g^{-1} = \begin{pmatrix} \mathbf{P}_g & \mathbf{Q}_g \\ \mathbf{R}_g & \mathbf{S}_g \end{pmatrix}^{-1} \tag{13}$$

$$= \begin{pmatrix} \mathbf{P}_g^{-1} + \mathbf{P}_g^{-1}\mathbf{Q}_g(\mathbf{M}_g/\mathbf{P}_g)^{-1}\mathbf{R}_g\mathbf{P}_g^{-1} & -\mathbf{P}_g^{-1}\mathbf{Q}_g(\mathbf{M}_g/\mathbf{P}_g)^{-1} \\ -(\mathbf{M}_g/\mathbf{P}_g)^{-1}\mathbf{R}_g\mathbf{P}_g^{-1} & (\mathbf{M}_g/\mathbf{P}_g)^{-1} \end{pmatrix}.$$

We define the four sub-matrices $\tilde{\mathbf{P}}_g$, $\tilde{\mathbf{Q}}_g$, $\tilde{\mathbf{R}}_g$ and $\tilde{\mathbf{S}}_g$ by

$$\tilde{\mathbf{P}}_g = \mathbf{P}_g^{-1} + \mathbf{P}_g^{-1}\mathbf{Q}_g(\mathbf{M}_g/\mathbf{P}_g)^{-1}\mathbf{R}_g\mathbf{P}_g^{-1} \tag{14}$$

$$\tilde{\mathbf{Q}}_g = -\mathbf{P}_g^{-1}\mathbf{Q}_g(\mathbf{M}_g/\mathbf{P}_g)^{-1} \tag{15}$$

$$\tilde{\mathbf{R}}_g = -(\mathbf{M}_g/\mathbf{P}_g)^{-1}\mathbf{R}_g\mathbf{P}_g^{-1} \tag{16}$$

$$\tilde{\mathbf{S}}_g = (\mathbf{M}_g/\mathbf{P}_g)^{-1}. \tag{17}$$

Rearranging those terms we get

$$\mathbf{P}_g^{-1} = \tilde{\mathbf{P}}_g - \tilde{\mathbf{Q}}_g\tilde{\mathbf{S}}_g^{-1}\tilde{\mathbf{R}}_g. \tag{18}$$

As, by hypothesis, we know the inverse $\mathbf{M}_g^{-1}$ of the global matrix, we are able to extract $\tilde{\mathbf{P}}_g$, $\tilde{\mathbf{Q}}_g$, $\tilde{\mathbf{R}}_g$ and $\tilde{\mathbf{S}}_g$ from the whole inverted matrix. Thus, the main cost to obtain the inverse of $\mathbf{P}_g$ of size $p \times p$ becomes the one of inverting $\tilde{\mathbf{S}}_g$ whose size is $q \times q$. In the first approximation, if the number of measurements to suppress is smaller than the number of remaining ones, this methods gives a notable gain. As soon as the matrix $\mathbf{P}_g^{-1} = \mathbf{M}_n^{-1}$, the final calculation of $\mathbf{K}_n$ is straightforward.

To highlight the advantages of this method with respect to the standard inversion of sub-matrix, some tests are shown on a 4000×4000 full semi-definite positive regular matrix. The curves showing the effective computing time in the percentage of the computing time of the full matrix are presented in Fig. 6.

Fig. 6 shows that, when the sub-matrix has roughly the size of the initial matrix, the inversion by Schur complement is far more efficient than the direct inversion. Above around 60% of the size of the initial matrix, the direct inversion becomes more efficient. The crossing point is at 60% instead of 50%, as expected in the first approximation. This difference comes from the few additional multiplications that need to be done in the Schur complement calculation, as we can see in Eq. (12). Globally, we see that the most efficient method is to use a hybrid calculation that chooses the best way to make the calculation as a function of the number of measurements removed. To quantify the improvement of such a hybrid choice, we integrate the curves of direct inversion and compare it to the integral of hybrid option (minimum of both cases) within the instrument loss range. The ratio in percentage of both integrals shows that benefit of this hybrid method represents an overall gain of 64% with respect to the standard method.

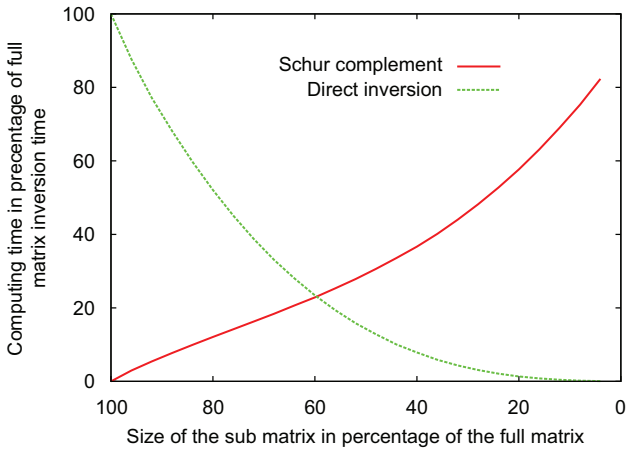

Fig. 6. Calculation time as a function of the size of the sub-matrix. Calculation time is given as a percentage of the calculation time of the full size matrix. The size of the sub-matrix is given as a percentage of the size of the full matrix. The curves in full line (red) and in dashed line (green) represent the inversion by Schur complement and direct inversion respectively. (For interpretation of the references to color in this figure legend, the reader is referred to the web version of this article.)

References

[1] S. Massart, S. Buis, P. Erhard, G. Gacon, Nuclear Science and Engineering 155 (3) (2007) 409.
[2] D.F. Parrish, J.C. Derber, Monthly Weather Review 120 (1992) 1747.
[3] R. Todling, S.E. Cohn, Monthly Weather Review 122 (1994) 2530.
[4] K. Ide, P. Courtier, M. Ghil, A.C. Lorenc, Journal of the Meteorological Society of Japan 75 (1B) (1997) 181.
[5] S.M. Uppala, et al., Journal of the Royal Meteorological Society 131 (612, Part B) (2005) 2961.
[6] E. Kalnay, et al., Bulletin of American Meteorological Society 77 (1996) 437.
[7] G.J. Huffman, et al., Bulltin of American Meteorological Society 78 (1997) 5.
[8] O. Talagrand, Journal of the Meteorological Society of Japan 75 (1B) (1997) 191.
[9] E. Kalnay, Atmospheric Modeling, Data Assimilation and Predictability, 2003.
[10] F. Bouttier, P. Courtier, Data assimilation concepts and methods, in: Meteorological Training Course Lecture Series, ECMWF, March, 1999.
[11] F. Rabier, H. Järvinen, E. Kilnder, J. Mahfouf, A. Simmons, Quarterly Journal of the Royal Meteorological Society 126 (2000) 1143–1170.
[12] J.J. Duderstadt, L.J. Hamilton, Nuclear Reactor Analysis, John Wiley and Sons, 1976.
[13] G. Matheron, La théorie des variables régionalisées et ses applications Cahiers du Centre de Morphologie Mathématique de l'ENSMP, Fontainebleau, Fascicule 5, 1970.
[14] D. Marcotte, Géologie et gèostatistique minières (lecture), 2008.
[15] J.-P. Argaud, B. Bouriquet, P. Erhard, G. Gacon, S. Massart, Exploitation optimale des mesures neutroniques pour l'évaluation de l'état des coeurs de centrales nucléaires, in: SFP Conference, 9–13 July 2007.
[16] J.-P. Argaud, B. Bouriquet, P. Erhard, S. Massart, S. Ricci, Data assimilation in nuclear power plant core, in: ECMI Conference, London, 30 June–4 July 2008, IMA, 2008.
[17] F. Zhang, The Schur Complement and its Applications, Springer, 2005.